Inorganic Chemistry
Article

Inorg. Chem. **2011**, *50*, 559–564 **559**
DOI: 10.1021/ic101875r

A Giant Polyaluminum Species S−Al_{32} and Two Aluminum Polyoxocations Involving Coordination by Sulfate Ions S−Al_{32} and S−K−Al_{13}

Zhong Sun,*,† Hui Wang,† Honggeer Tong,‡ and Shaofan Sun†

†*College of Chemistry and Chemical Engineering, Inner Mongolia University, 235 West University Road, Hohhot 010021, China, and* ‡*Inner Mongolia Mineral Testing Institute, 16 Zhaojun Road, Hohhot 010031, China*

Received September 12, 2010

The giant polyaluminum species $[Al_{32}O_8(OH)_{60}(H_2O)_{28}(SO_4)_2]^{16+}$ (S−Al_{32}) and $[Al_{13}O_4(OH)_{25}(H_2O)_{10}(SO_4)]^{4+}$ (S−K−Al_{13}) [S means that sulfate ions take part in coordination of the aluminum polycation; K represents the Keggin structure] were obtained in the structures of $[Al_{32}O_8(OH)_{60}(H_2O)_{28}(SO_4)_2][SO_4]_7[Cl]_2\cdot 30H_2O$ and $[Al_{13}O_4(OH)_{25}(H_2O)_{10}(SO_4)]_4[SO_4]_8\cdot 20H_2O$, respectively. They are the first two aluminum polyoxocations coordinated by sulfate ions. The "core-shell" structure of S−Al_{32} is similar to that of Al_{30}, but the units are linked by two $[Al(OH)_2(H_2O)_3(SO_4)]^-$ groups with replacement of four η^1-H_2O molecules. The structure of S−K−Al_{13} is similar to the well-known structure of ε-K−Al_{13}, but the units are linked by two $(SO_4^{2-})_{0.5}$ with replacement of a H_3O^+ ion. It was shown that strong interaction exists between the polyoxocations and counterions. On the basis of their structural features and preparation conditions, a formation and evolution mechanism (from ε-K−Al_{13} to S−K−Al_{13} and S−Al_{32}) has been proposed. A local basification degree symmetrical equalization principle was extracted based on a comparison of the calculated results of the local basification degree for each central Al^{3+} ion included in a polycation. They can be used to explain how the two aluminum species are formed and evolved and why the sulfate ions can coordinate to them and to predict where the OH-bridging positions will be upon further hydrolysis.

Introduction

The solution chemistry of Al^{III}, especially the hydrolytic chemistry, has become the focus of attention and a hot research area in many academic fields such as geochemistry, environmental science, biochemistry, medicine, and water treatment.[1−7] Aluminum species play a critical role in the study of the transport and transformation law of aluminum in soil and natural water. For example, Furrer et al. showed that the amorphous aluminum oxyhydroxide flocs in streams probably form from aggregation of ε-K−Al_{13},[8] which was often used as a structural model for discussing related issues in geochemistry. Phillips et al. determined the rates of oxygen exchange of the complex and found that the rates of hydroxyl exchange are extremely sensitive to subtle differences in the local structure and Brønsted acidity of the surface.[9] Rustad et al. detailed the pathways and explained why the exchange rates are so sensitive to single-atom substitution.[10] Hunter and Ross found that polynuclear aluminum species are more toxic than mononuclear species and the ε-K−Al_{13} species can make a significant contribution to the toxicity of aluminum in forested spodosol soils.[11] A study on the formation and evolution process of aqueous aluminum species is of great significance for a deep understanding of the formation process and the action mechanism of polyaluminum flocculants on the surfaces of the colloidal particles and for an objective selection of highly efficient flocculants in the water treatment field.[12]

*To whom correspondence should be addressed. E-mail: cesz2008@126.com. Fax: +86 471 4992981.

(1) Casey, W. H. *Chem. Rev.* **2006**, *106*, 1–16.
(2) Bi, S. P.; Wang, C. Y.; Cao, Q.; Zhang, C. H. *Coord. Chem. Rev.* **2004**, *248*, 441–455.
(3) Swaddle, T. W.; Rosenqvist, J.; Yu, P.; Bylaska, E.; Phillips, B. L.; Casey, W. H. *Science* **2005**, *308*, 1450–1453.
(4) Tang, H. X. *Inorganic Polymer Flocculation Theory and Flocculants*; China Architecture & Building Press: Beijing, 2006.
(5) Jolivet, J. P.; Henry, M.; Livage, J. *Metal Oxide Chemistry and Synthesis: From Solution to Solid State*; John Wiley & Sons: Chichester, U.K., 2000.
(6) Bertsch, P. M.; Parker, D. R. *Aqueous Polynuclear Aluminum Species: The Environmental Chemistry of Aluminum*, 2nd ed.; CRC Press: Boca Raton, FL, 1996.
(7) Hsu, P. H. *Aluminum Hydroxides and Oxyhydroxide: Minerals in Soil Environments*, 2nd ed.; Soil Science Society of America Book Series 1; Soil Science Society of America: Madison, WI, 1989.
(8) Furrer, G.; Phillips, B. L.; Ulrich, K.-U.; Pöthig, R.; Casey, W. H. *Science* **2002**, *297*, 2245–2447.
(9) Phillips, B. L.; Casey, W. H.; Karlsson, M. *Nature* **2000**, *404*, 379–382.
(10) Rustad, J. R.; Loring, J. S.; Casey, W. H. *Geochim. Cosmochim. Acta* **2004**, *68*, 3011–3017.
(11) Hunter, D.; Ross, D. S. *Science* **1991**, *251*, 1056–1058.
(12) Stewart, T. A.; Trudell, D. E.; Alam, T. M.; Ohlin, C. A.; Lawler, C.; Casey, W. H.; Jett, S.; Nyman, M. *Environ. Sci. Technol.* **2009**, *43*, 5416–5422.

Published on Web 12/15/2010

Since the idea of the possible existence of an aluminum polymeric species was introduced in 1931,[13] many research papers have reported on the reaction process of hydrolysis and polymerization, the distribution, and the formation and transformation mechanism of various aqueous aluminum species. However, because the reaction process is so complicated, up to now a consensus has still not been reached, yet the hydrolytic chemistry of Al^{III} remains poorly understood.[3,14]

In order to study the aluminum species, many research methods have been developed such as aluminum−ferron complexation-timed spectrophotometry,[15,16] ^{27}Al NMR spectrometry,[17,18] and mass spectrometry.[19,20] However, these methods are not comparable with crystal structure analysis because of their limitations. Because the Al^{III} hydroxyl polymeric species in a single crystal are formed under specified conditions, they may not be observable in common aqueous solution chemistry.[1,4] So, the best way is to obtain pure polyaluminum compounds and solve their crystal structures.

Although the polyaluminum species have been studied for a century, only six species have been identified based on the results of crystal structure analysis.[21−30] The polyhedral representation (Figure S1 in the Supporting Information) and the classification of these structures are given in the Supporting Information. Almost all species among them are crystallized as sulfates (or selenates), except P−Al_{13}, which crystallized as chloride and nitrate. However, those sulfate (or selenate) ions appear in the interstices between the polyoxocations only, indicating that an aluminum polyoxocation coordinated by SO_4^{2-} (or SeO_4^{2-}) ions has never been observed.

Our group has prepared more than 20 crystals from hydrolyzed aluminum solutions such as $Al_5(OH)_{12}(H_2O)_4Cl_3$, $Al_5(OH)_{12}(H_2O)_{7.5}Cl_3$, $Al_9(OH)_{21}(H_2O)_{18}Cl_6$, $Al_{13}(OH)_{24}(H_2O)_{37}Cl_{15}$, $Al_{17}O_{16}(OH)_{16}Cl_3$, $Al_{24}O_{11}(OH)_{44}Cl_6$, $Al_{29}(OH)_{78}Cl_9$, AlOOH, etc.[31−40] Eight of them were verified as new species by X-ray diffraction. Four of them were characterized by single-crystal X-ray structure analysis.[41] In this paper, we first report the two crystal structures of $[Al_{32}O_8(OH)_{60}(H_2O)_{28}(SO_4)_2][SO_4]_7[Cl]_2\cdot 30H_2O$ and $[Al_{13}O_4(OH)_{25}(H_2O)_{10}(SO_4)]_4[SO_4]_8\cdot 20H_2O$ coordinated by SO_4^{2-} besides O^{2-}, OH^-, and H_2O and then study their structural features and the formation and evolution mechanism. To our knowledge, the polyoxocation $[Al_{32}O_8(OH)_{60}(H_2O)_{28}(SO_4)_2]^{16+}$ (S−Al_{32}) should be the biggest one so far. Similar polyoxocation $[Al_{13}O_4(OH)_{25}(H_2O)_{10}(SO_4)]^{4+}$ (S−K−Al_{13}) will be discussed too. These two aluminum polyoxocations should be the first two cases involving coordination by sulfate ions.

Experimental Details

Synthesis. A NaOH solution (0.25 mol/L) was added dropwise into an $AlCl_3$ solution (0.25 mol/L) at 70 °C under fast stirring, and the solution were maintained at 70 °C for 36 h. Then the solution obtained with $B = 2.5$ (B = [OH]/[Al] reflecting the basification degree of the medium) was separated into two parts (A and B). The solution A was heated to 150 °C in a steel reactor with a Teflon inner container and aged for 8 h. After cooling to room temperature, a Na_2SO_4 solution (0.24 mol/L) was added into the solution up to $m = 0.30$ (m = [SO_4]/[Al]). After 1 week, colorless platelike single crystals (crystal A) were obtained. Solution B was kept at 70 °C, and a Na_2SO_4 solution (0.24 mol/L) was added dropwise up to $m = 0.50$; then the solution was cooled to room temperature. After 5 days, colorless prismatic single crystals (crystal B) were obtained.

Single-Crystal X-ray Structure Analysis. Two fragments of crystals A and B were selected for structure analysis. Diffraction intensities were recorded on a Bruker SMART APEX-II X-ray diffractometer (graphite monochromator, CCD area detector), multiscan absorption corrections were applied by using *SADABS*,[42] and the diffraction data were reduced by using Bruker *SAINT*.[43] Their initial structures were solved by direct methods using *SHELXS-97*,[43] and the coordinates of the rest of the non-H atoms were obtained from difference Fourier maps. All coordinates and anisotropic thermal parameters of the non-H atoms were refined by full-matrix least-squares techniques based on F^2 using *SHELXL-97*.[43] All coordinates of H atoms were generated geometrically, so their position and isotropic thermal parameters were constrained. All SO_4^{2-} ions in crystal B were restrictively refined as rigid groups. The main crystallographic parameters and the X-ray data for these two compounds are listed in Table 1. The structures of the polyoxocations S−Al_{32} and S−K−Al_{13} are shown in Figures 1 and 3, and the distributions in their unit cells are shown in Figures 2 and 4, respectively.

(13) Jander, G.; Winkel, A. Z. *Inorg. Chem.* **1931**, *200*, 257–278.
(14) Pascual-Cosp, J.; Artiaga, R.; Corpas-Iglesias, F.; Benítez-Guerrero, M. *Dalton Trans.* **2009**, 6299–6308.
(15) Smith, R. W. *Adv. Chem. Ser.* **1971**, *106*, 250–256.
(16) Wang, C. Y.; Zhang, C. H.; Bi, S. P.; Zhang, Z. C.; Yang, W. H. *Chin. J. Spectrosc. Spectroanal.* **2005**, *25*, 252–256.
(17) Allouche, L.; Huguenard, C.; Taulelle, F. *J. Phys. Chem. Solids* **2001**, *62*, 1525–1531.
(18) Müller, V. D.; Gessner, W.; Schönherr, S.; Görz, H. *Z. Anorg. Allg. Chem.* **1981**, *483*, 153–160.
(19) Zhao, H.; Liu, H. J.; Qu, J. H. *J. Colloid Interface Sci.* **2009**, *330*, 105–112.
(20) Sarpola, A. *The Hydrolysis of Aluminium: A Mass Spectrometric Study*; Oulu University Press: Oulu, Finland, 2007.
(21) (a) Johansson, G. *Acta Chem. Scand.* **1960**, *14*, 771–773. (b) Johansson, G.; Lundgren, G.; Sillén, L. G.; Söderquist, R. *Acta Chem. Scand.* **1960**, *14*, 769–771. (c) Johansson, G. *Ark. Kemi* **1963**, *20*, 305–319.
(22) Johansson, G. *Ark. Kemi* **1963**, *20*, 321–342.
(23) Rowsell, J.; Nazar, L. F. *J. Am. Chem. Soc.* **2000**, *122*, 3777–3778.
(24) Allouche, L.; Gérardin, C.; Loiseau, T.; Férey, G.; Taulelle, F. *Angew. Chem.* **2000**, *112*, 521–524.
(25) Son, J.-H.; Kwon, Y.-U.; Han, O. H. *Inorg. Chem.* **2003**, *42*, 4153–4159.
(26) Seichter, W.; Mögel, H. J.; Brand, P.; Salah, D. *Eur. J. Inorg. Chem.* **1998**, 795–797.
(27) Gatlin, J. T.; Mensinger, Z. L.; Zakharov, L. N.; Maclnnes, D.; Johnson, D. W. *Inorg. Chem.* **2008**, *47*, 1267–1269.
(28) Heath, S. L.; Jordan, P. A.; Johnson, I. D.; Moore, G. R.; Powell, A. K.; Helliwell, M. *J. Inorg. Biochem.* **1995**, *59*, 785–794.
(29) Casey, W. H.; Olmstead, M. M.; Phillips, B. L. *Inorg. Chem.* **2005**, *44*, 4888–4890.
(30) Johansson, G. *Acta Chem. Scand.* **1962**, *16*, 403–420.
(31) Wang, R. F.; Sun, Z.; Zhang, Y. *Chin. J. Appl. Chem.* **2009**, *26*, 878–880.
(32) Du, S. Y.; Wang, H.; Sun, Z. *J. Environ. Sci. Eng.* **2009**, *3*, 47–52.
(33) Du, S. Y.; Sun, Z.; Wang, H. *J. Environ. Sci. Eng.* **2009**, *3*, 40–42,52.
(34) Du, S. Y.; Sun, Z.; Wang, H. *J. Chem. Chem. Eng.* **2008**, *2*, 16–19.
(35) Meng, Y. F.; Sun, Z.; Wang, H.; Feng, H. J. *J. Chem. Chem. Eng.* **2008**, *2*, 25–28.
(36) Meng, Y. F.; Sun, Z.; Wang, H.; Yu, N. N. *J. Environ. Sci. Eng.* **2008**, *2*, 15–17.
(37) Du, S. Y.; Sun, Z.; Wang, H. *J. Environ. Sci. Eng.* **2008**, *2*, 30–32.
(38) Sun, Z. Chinese Invention Patent ZL200510064782.6, 2007.
(39) Sun, Z.; Zhao, H. D.; Yang, X. S.; Zhu, F. Z. *Chin. J. Environ. Chem.* **2007**, *26*, 31–34.
(40) Fei, Y. L.; Sun, Z.; Wang, R. F.; Tong, H. G. E.; Zhang, B. L. C. K. *Nat. Sci. Res.* **2007**, *10*, 65–67.
(41) Sun, Z.; Zhao, H. D.; Tong, H. G. E.; Wang, R. F.; Zhu, F. Z. *Chin. J. Struct. Chem.* **2006**, *25*, 1217–1227.
(42) Sheldrick, G. M. *SADABS: Siemens Area Detector Absorption Correction*; University of Göttingen: Göttingen, Germany, 2008.
(43) Sheldrick, G. M. *SHELXTL: Bruker Analytical X-ray Systems*; Madison, WI, 2008.

Table 1. Main Crystallographic Parameters and X-ray Data for Crystals A and B

	crystal A	crystal B		crystal A	crystal B
empirical formula	$Al_{32}Cl_2H_{176}O_{162}S_9$	$Al_{52}H_{220}O_{224}S_{12}$	abs coeff (mm^{-1})	0.536	0.554
fw	3992.21	5593.44	λ(Mo Kα) (Å)	0.710 73	0.710 73
cryst syst	triclinic	monoclinic	limiting indices	$-17 \leq h \leq +15$	$-20 \leq h \leq +24$
temp (K)	296(2)	296(2)		$-19 \leq k \leq +19$	$-13 \leq k \leq +13$
space group	$P\bar{1}$ (No. 2)	$P2/c$ (No. 13)		$-19 \leq l \leq +19$	$-27 \leq l \leq +13$
a (Å)	14.949(3)	20.799(7)	range of θ (deg)	1.39−24.50	1.17−25.00
b (Å)	16.384(3)	11.637(4)	all/unique refIns/R_{int}	20 194/11 601/0.1248	22 636/8183/0.0995
c (Å)	17.055(3)	22.864(6)	completeness (%)	99.2	99.9
α (deg)	66.79(3)		data/restraints/param	11 601/253/929	8183/206/670
β (deg)	70.35(3)	122.99(2)	obsd refIns [$I > 2\sigma(I)$]	4301	3736
γ (deg)	70.32(3)		GOF on F^2 [$I > 2\sigma(I)$]	0.910	1.059
volume (Å^3)	3513.4(15)	4642(3)	GOF on F^2 (all data)	0.909	1.089
Z	1	1	R indices [$I > 2\sigma(I)$]	$R = 0.1158$, $wR = 0.0985$	$R = 0.0904$, $wR = 0.1378$
D_c (g/cm^3)	1.887	2.001	R indices (all data)	$R = 0.2015$, $wR = 0.1231$	$R = 0.2210$, $wR = 0.1649$
F(000)	2066	2880	largest difference peak/hole (e/Å^3)	1.062/−0.741	0.911/−0.558
crystal size (mm^3)	0.20 × 0.18 × 0.18	0.20 × 0.18 × 0.16	residual electron density (e/Å^3)	0.141	0.119

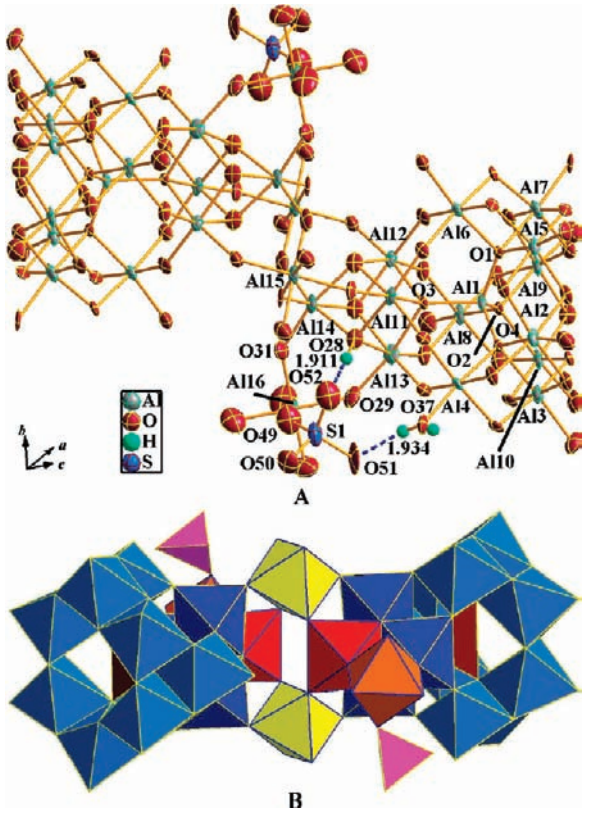

Figure 1. Ionic structure of S−Al_{32} species $[Al_{32}O_8(OH)_{60}(H_2O)_{28}(SO_4)_2]^{16+}$: (A) Ellipsoid−stick representation with a probability of 80%. Only those atoms involved in the Results and Discussion section are labeled, and the intramolecular hydrogen bonds lengths (Å) are marked. (B) Polyhedral representation. Color code: brown, AlO_4; pink, SO_4; others, AlO_6.

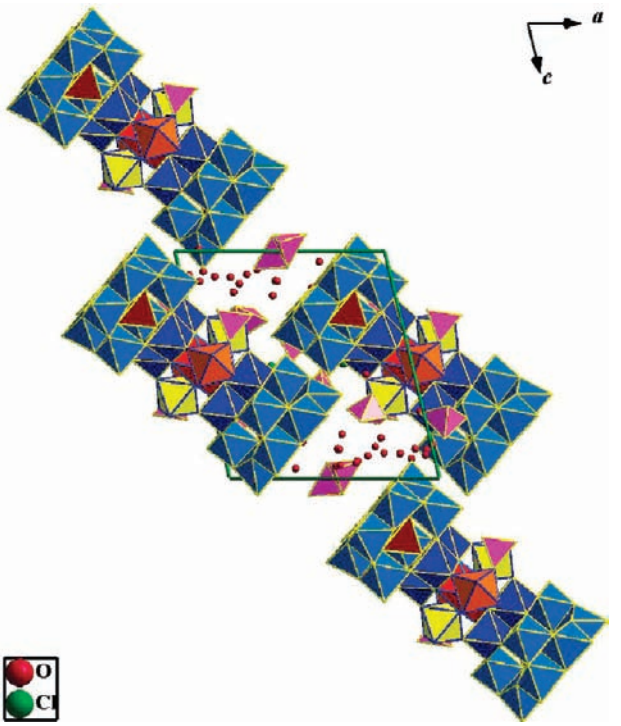

Figure 2. Distribution of S−Al_{32} polyoxocations in the unit cell; a view along the b axis.

Results and Discussion

Polyoxocation S−Al_{32} is centrosymmetric about its barycenter; see Figure 1. Its structure is similar to that of Al_{30}, but the units are linked by two $[Al(OH)_2(H_2O)_3(SO_4)]^-$ groups with replacement of four η^1-H_2O molecules. Each of the groups is suspended on the two coordination sites, O29 and O31, as marked in Figure 1A, between the AlO_6 monomer "cap" (red octahedron) and the rotated triad (the blue Al_3O_{13} unit) by vertex sharing in each half of S−Al_{32}, resulting in a triangle-reinforced structure around each "cap" and a giant aluminum polyoxocation $[Al_{32}O_8(OH)_{60}(H_2O)_{28}(SO_4)_2]^{16+}$ (S−Al_{32}). The orientation of each coordinated sulfate ion is decided by two intramolecular hydrogen bonds (O28−H28···O52 = 1.911 Å and O37−H···O51 = 1.934 Å, as marked in Figure 1A).

It is clearly seen from Figure 2 that all S−Al_{32} polyoxocations have the same orientation and their barycenters are located on the centers of all {100} lattice planes. A total of 7 uncoordinated SO_4^{2-}, 2 Cl^- anions, and 30 H_2O molecules, which are split and disordered popularly, intersperse among the interstices of S−Al_{32} polyoxocations, so there is one $[Al_{32}O_8(OH)_{60}(H_2O)_{28}(SO_4)_2][SO_4]_7[Cl]_2 \cdot 30H_2O$ molecule in each unit cell only. One of the uncoordinated SO_4^{2-} ions locates nearby the symcenter, at ($^1/_2$, 0, 0), which is split into halves connected by edge sharing with an S−S distance of 2.02 Å. The S−S distance is much longer than that of 1.45 Å

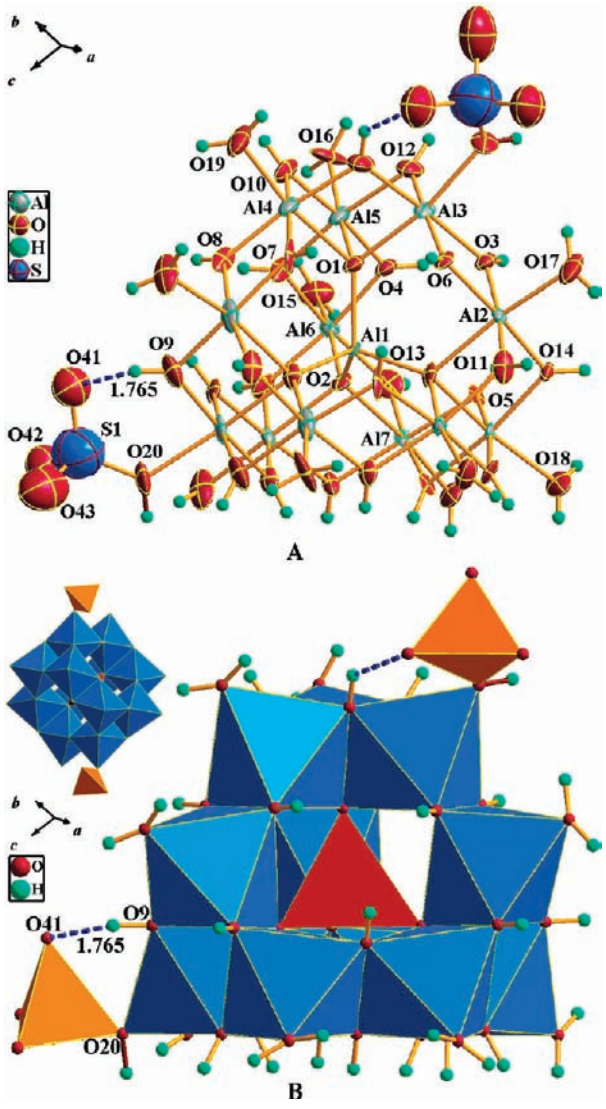

Figure 3. (A) Ellipsoid−stick representation with a probability of 50%. Only those atoms in the asymmetric unit are labeled, and the intramolecular hydrogen bond length (Å) is marked. (B) Polyhedral representation, with the inset showing a view along the *b* axis. Color code: brown, AlO_4; light blue, AlO_6; orange, $(SO_4)_{0.5}$.

in Al_{30} reported by Allouche et al., in which an uncoordinated SO_4^{2-} ion is placed near the 2 axis.[24]

The structure of the S−K−Al_{13} species is similar to that of ε-K−Al_{13} (see Figure 3), but the units are linked by two $(SO_4^{2-})_{0.5}$ with replacement of a H_3O^+ ion; i.e., on the sites occupied by a pair of the 12 nonshared η^1-OH_2 molecules, which are related by the 2 axis in a ε-K−Al_{13} cluster, the two H_3O^+ semiions are taken off because of further hydrolysis and the two SO_4^{2-} semiions are connected simultaneously. The orientation of each coordinated sulfate semiion is decided by a strong intramolecular hydrogen bond (O9−H···O41 = 1.765 Å, as marked in Figure 3), so two OH^- semiions remain statistically, resulting in a K−Al_{13}-like structure with symmetry C_2 and the structural formula $[(SO_4)_{0.5}(OH)_{0.5}Al_6(OH)_{12}(H_2O)_5AlO_4Al_6(OH)_{12}(H_2O)_5(OH)_{0.5}(SO_4)_{0.5}]^{4+}$ (namely, S−K−Al_{13}), which should be helpful for understanding the two K−Al_{13}-like structures with 25 OH^- ligands in $[Al_{13}O_4(OH)_{25}(H_2O)_{11}][Cl]_6\cdot xH_2O$ and $[Al_{13}O_4(OH)_{25}(H_2O)_{11}][SO_4]_3\cdot 16H_2O$.[18,22]

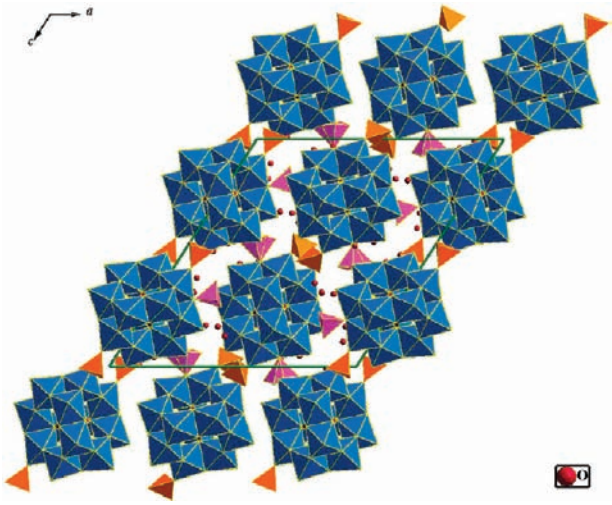

Figure 4. Distribution of S−K−Al_{13} species in a unit cell; a view along the *b* axis. Color code: pink, SO_4.

It is seen obviously from Figure 4 that the S−K−Al_{13} species in the unit cell have different orientations. A pair of them, which have similar structural parameters but different orientations [their barycenters are placed on the 2 axes at ($^1/_2$, *y*, $^1/_4$) and (0, *y*, $^1/_4$), respectively], are operated by the *c* glide plane located at $y = {}^1/_2$, producing another pair of S−K−Al_{13} [their barycenters are placed on the 2 axes at ($^1/_2$, *y*, $^3/_4$) and (0, *y*, $^3/_4$), respectively]. Under the symmetry operation of space group $P2/c$, 2 uncoordinated SO_4^{2-} ions and 5 H_2O molecules in an asymmetric unit can produce 8 SO_4^{2-} ions and 20 H_2O molecules in total, which are split and disordered mostly and filled in the interstices between the S−K−Al_{13} species. In total, there are four $[Al_{13}O_4(OH)_{25}(H_2O)_{10}(SO_4)][SO_4]_2\cdot 5H_2O$ fragments, which have similar structure but different orientations; they form a structural motif $[Al_{13}O_4(OH)_{25}(H_2O)_{10}(SO_4)]_4[SO_4]_8\cdot 20H_2O$ in the unit cell, so the lattice is still a simple *P* form ($Z = 1$).

Single-crystal X-ray structure analysis is the best way to understand the structures of polyaluminum species, and it was widely employed to precipitate the dominant species from a hydrolyzed aluminum salt solution with sulfate or selenate counterions. In this way, the structures such as ε-K−Al_{13}, δ-K−Al_{13}, and Al_{30} species were determined unambiguously.[21−24] From those reports, all sulfate (or selenate) ions are only distributed in the interstices between the polyoxocations; not one is connected to an aluminum polyoxocation. Because of the appearance of the cases that aluminum polyoxocations can be coordinated by sulfates ions, it brings us much revelation.

First, because the strong interaction exists between the polyoxocations and the counterions, SO_4^{2-} ions can connect to an aluminum polyoxocation under proper conditions such as the aging temperature and aging time. In fact, it was found that a NaO_6 octahedron can cap on the rotated triad unit of the δ-K−Al_{13} cluster by sharing three of its edges in the structure of the Na−δ-Al_{13} species reported by Rowsell and Nazar. Such a strong interaction suggests that it may play a role in the ε → δ transformation,[23] so that the structural formula of Na−δ-Al_{13} can be rewritten as $[Na{-}\delta\text{-}Al_{13}O_4(OH)_{24}(H_2O)_{15}]^{8+}$. Another similar example can be found in Zunyite, in which 12 μ_2-OH groups on an α-K−Al_{13} cluster are averagely replaced by a 12-dentate chelating ligand

Table 2. Some B_l Values in S−Al_{32} and B_i Values of Several Polyaluminum Species

	numbers of various ligands					
central atom	μ_4-O	μ_3-OH	μ_2-OH	η^1-OH_2	μ_2-O(SO_4^{2-})	B_l
Al1	4					2.00
Al2−Al10	1		4	1		2.50
Al11−Al12	1	2	3			2.67
Al13 in Al_{30}	1	2	2	1		2.17
Al13	1	2	3			2.67
Al14 in Al_{30}		3	2	1		2.00
Al14		3	3			2.50
Al15			4	2		2.00
Al16 in Al_{32}[a]			2	4		1.00
Al16			2	3	1	2.00

	numbers of various ligands					
species	μ_4-O	μ_3-OH	μ_2-OH	η^1-OH_2	μ_2-O(SO_4^{2-})	B_i
Al_{30}	8	6	50	26		2.40
Al_{32}[a]	8	6	54	28		2.38
S−Al_{32}	8	6	54	28	2	2.44
ε-K−Al_{13}	4		24	12		2.46
Na−δ-Al_{13}	4	3	21	15		2.46
$Al_{13}(OH)_{25}$[b]	4		25	11		2.54
S−K−Al_{13}	4		25	10	1	2.62

[a] If SO_4^{2-} ions were not connected. [b] References 18 and 22.

$[SiO_4(SiO_3)_4]^{12-}$, which coordinates to six α-K−Al_{13} clusters, and each α-K−Al_{13} is coordinated by six $[SiO_4(SiO_3)_4]^{12-}$ polyanions.[44]

Second, the sulfate ions appear in pairs on two symmetric unbridged sites originally occupied by η^1-OH_2 molecules, and they prefer to coordinate to those Al^{3+} ions that show the most unequalized local basification degree compared with the internal basification degree of the whole aluminum polyoxocation. The local basification degree (B_l) refers to the actually shared [OH]/[Al] molar ratio for every central Al^{3+} ion in a polycation reflecting the hydrolysis degree of an individual Al^{3+} ion in a polycation. For example, Al14 [the center of the octahedral cap; see Figure 1A] is coordinated by three μ_3-OH and three μ_2-OH ligands in S−Al_{32}, its $B_l = 3/3 + 3/2 = 2.50$. The internal basification degree (B_i) means the [OH]/[Al] molar ratio for a polycation reflecting the hydrolysis degree of the whole polycation. Other ligands can be converted into OH^- groups easily, for example, one O^{2-} ligand converts two OH^- groups, one SO_4^{2-} converts one OH^- because only the μ_2-O atom is shared by Al and S atoms, and one η^1-OH_2 converts zero OH^- because it is not shared. There are 60 OH^-, 8 O^{2-}, 2 SO_4^{2-}, and 28 H_2O ligands in total in S−Al_{32}; they coordinate to 32 Al^{3+} ions, so its $B_i = (60 + 8 \times 2 + 2)/32 = 2.44$. On the basis of the definitions above, some calculated B_l values in S−Al_{32} and the B_i values of several polyaluminum species are listed in Table 2.

It is seen from Table 2 that the difference between the B_i of S−Al_{32} and the B_l of Al16 is small (2.44 − 2.00 = 0.44). However, if the SO_4^{2-} ion was not coordinated to it, the number of unbridged η^1-OH_2 ligands on Al16 would reach four, and its B_l value would decrease to 1.00, which is far below 2.38 (the internal basification degree of the imaginary Al_{32}), causing a large unequalized local basification degree (2.38 − 1.00 = 1.38). So, the unequalized local basification degree is the main reason why sulfate ions connect to the polyoxocation. In other words, a local basification degree symmetrical equalization (LBDSE) principle acts an important role for explaining and predicting the most possible OH-bridging position where further hydrolysis and polymerization reaction will happen. Moreover, the LBDSE principle can also be used to predict the evolution from Al_{30} to S−Al_{32}. As shown in Table 2, octahedral Al11, Al12, and Al13 are members of the rotated triad unit of the δ-K−Al_{13} cluster, and octahedral Al14 is the cap of the triad, forming a big tetrahedral unit. They should have similar coordination environments symmetrically. If the octahedral Al16 does not suspend (just as in Al_{30}), their B_l values are quite unequalized (2.67 for Al11 and Al12, 2.17 for Al13, and 2.00 for Al14). After suspending and subsequently connecting to a SO_4^{2-} ion, their unequalized local basification degrees are observably improved (2.67 for Al13 and 2.50 for Al14). That is, the four unbridged η^1-H_2O molecules on Al13 and Al14 as well as their equivalent atoms in Al_{30} have the strongest reactivity, which is in good conformity with the result of the molecular dynamics simulation calculation for Al_{30} by Rustad; in this report, the four η^1-H_2O molecules exhibit the strongest acidity.[45] Also, our result is also consistent with the results of the oxygen exchange rates for Al_{30} determined by Phillips et al., in which four of the 26 η^1-H_2O molecules are exchanged so fast that they cannot be resolved.[46] On the basis of the above investigation and discussion about the local basification degree, it is becoming more clear that the LBDSE principle can be expressed as that in a relatively stable polymeric aluminum species; those Al^{3+} ions having identical or similar symmetry would have identical or similar local basification degrees and coordination environments. In this way, the driving force for the formation and evolution of the two aluminum species and the reason why the sulfate ions can coordinate to the specified positions instead of anywhere can be explained. Also, the OH-bridging positions upon further hydrolysis can also be predicted.

Finally, the aging temperature is the most important influencing factor. By analysis and comparison of the hydrolysis reaction conditions with those of Rowsell and Nazar[23] and Allouche et al.,[24] we found that the aging temperature plays a critical role in the formation of aluminum polyoxocation. For example, if the S−K−Al_{13} species were prepared under lower aging temperature (70 °C), it should be the most adjacent precursor of the Na−δ-Al_{13} species; if the S−Al_{32} species were prepared under higher aging temperature (150 °C), it should be the most adjacent derivative of the Al_{30} species. On the basis of such a view of recognition, a formation and evolution mechanism from ε-K−Al_{13} to S−K−Al_{13} and S−Al_{32} is speculated, as shown in Figure 5. From the mechanism, the SO_4^{2-} ion may be regarded as an internal basification degree regulator to suit the changes of the basification degree of the hydrolyzed solution by connecting to a polyoxocation or disconnecting from it. Combining the formation and evolution mechanism with the LBDSE principle, it may be predicted that those sites occupied (or ever occupied) by SO_4^{2-} ions (or semiions) would be the OH-bridging positions to other bigger or smaller aluminum species upon further hydrolysis. In other words, where a sulfate ion was connected is where a OH bridging would happen. So, the

(44) Pauling, L. *Z. Kristallogr.* **1933**, *84*, 442–452.

(45) Rustad, J. R. *Geochim. Cosmochim. Acta* **2005**, *69*, 4397–4410.

(46) Phillips, B. L.; Lee, A.; Casey, W. H. *Geochim. Cosmochim. Acta* **2003**, *67*, 2725–2733.

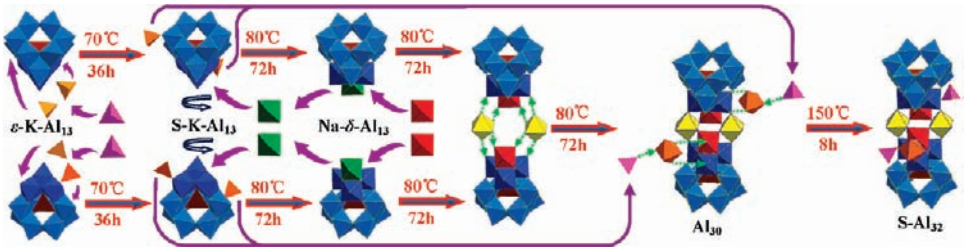

Figure 5. Speculative formation and evolution mechanism from ε-K−Al_{13} to S−K−Al_{13} and S−Al_{32}. Color code: brown, AlO_4; pink, SO_4; orange tetrahedron, $(SO_4)_{0.5}$; green, NaO_6; others, AlO_6.

SO_4^{2-} ion coordinated to an aluminum polyoxocation can also be regarded as a predictor for further hydrolysis.

Conclusion

A giant polyaluminum species S−Al_{32} and two aluminum polyoxocations involving coordination by sulfate ions S−Al_{32} and S−K−Al_{13} were observed. The ionic and crystal structures were described, and the structural features were discussed. The LBDSE principle and formation and evolution mechanism from ε-K−Al_{13} to S−K−Al_{13} and S−Al_{32} were proposed. They can be used to explain how the two aluminum species are formed and evolved and why the sulfate ions can coordinate to them and to predict where the OH-bridging positions will be upon further hydrolysis. Also, thereby the following viewpoints were derived: A strong interaction exists between the aluminum polyoxocations and the counterions; the sulfate ions appear in pairs on symmetric unbridged sites where the hydrogen bonds formed are the strongest, and they can be regarded as basification degree regulators and hydrolysis predictors; the further hydrolysis reaction for a primary aluminum species always occurs on those unbridged coordination positions where the local basification degrees are the most unequalized. S−K−Al_{13} should be the most adjacent precursor of Na−δ-Al_{13}, and S−Al_{32} should be the most adjacent derivative of the Al_{30} species. We believe that the research results of this paper are very important to obtaining a deep understanding of the formation and evolution process of aluminum species, to predicting the reaction positions of further hydrolysis, and to improving the current polymerization models in a hydrolyzed aluminum solution. They will have a great impact on many subjects closely related to the solution chemistry of Al^{III}, especially the hydrolytic chemistry, such as geochemistry, environmental science, biochemistry, medicine, and water treatment.

Acknowledgment. We are thankful for support from the National Natural Science Foundation Committee of China [NNSFC Grants 20563002 (to Z.S.) and 20967005 (to H.W.)].

Supporting Information Available: Crystallographic data in CIF format for $[Al_{32}O_8(OH)_{60}(H_2O)_{28}(SO_4)_2][SO_4]_7[Cl]_2 \cdot 30H_2O$, $[Al_{13}O_4(OH)_{25}(H_2O)_{10}(SO_4)]_4[SO_4]_8 \cdot 20H_2O$, and $[Al_{13}(OH)_{24}(H_2O)_{24}][Cl]_{15} \cdot 13H_2O$, a polyhedral representation (Figure S1), and classification of the structurally known polyaluminum species. This material is available free of charge via the Internet at http://pubs.acs.org. The CIFs may also be obtained from Fachinformationszentrum Karlsruhe, 76344 Eggenstein-Leopoldshafen, Germany [fax (+49)7247-808-666; e-mail crysdata@fiz-karlsruhe.de, web site http://www.fiz-karlsruhe.de/request_for_deposited_data.html] upon quoting the depository numbers CSD 421844, 421742, and 417024, respectively.